Emulsion Stabilization and Flocculation in CO_2. 1. Turbidimetry and Tensiometry

M. L. O'Neill, M. Z. Yates, K. L. Harrison, and K. P. Johnston*

Department of Chemical Engineering, The University of Texas at Austin, Austin, Texas 78712-1062

D. A. Canelas, D. E. Betts, and J. M. DeSimone*

Department of Chemistry, The University of North Carolina, Chapel Hill, North Carolina 27599-3290

S. P. Wilkinson

Air Products and Chemicals Inc., Allentown, Pennsylvania 18195-1501

Received November 18, 1996; Revised Manuscript Received April 14, 1997[⊗]

ABSTRACT: The stabilization and flocculation of emulsions of poly(2-ethylhexyl acrylate) (PEHA) in liquid and supercritical carbon dioxide (SC-CO_2) with the homopolymer poly(1,1-dihydroperfluorooctyl acrylate) (PFOA), the diblock copolymer polystyrene-*b*-PFOA, and the triblock copolymer PFOA-*b*-poly(vinyl acetate)-*b*-PFOA were quantified by turbidimetry and measurements of interfacial tension. Upon decreasing the CO_2 density, a distinct change in emulsion stability occurs at the critical flocculation density (CFD). Steric stabilization by the homopolymer PFOA is due to a small number of adsorbed segments and a large number of segments in loops and tails as determined by measurements of the PEHA−CO_2 interfacial tension. Below the CFD, flocculation is irreversible due to bridging by the high molecular weight PFOA chains. PS-*b*-PFOA adsorbs much more strongly to the PEHA−CO_2 interface than the other two stabilizers. Consequently, it provides the greatest resistance to emulsion flocculation, both above and below the CFD, and the most reversible flocculation. For all stabilizers studied, the CFD correlates very well with the estimated Θ point for PFOA in bulk CO_2.

Introduction

Although nonvolatile substances are typically insoluble in supercritical fluids (SCFs) such as ethane and CO_2, they may be dispersed into these fluids with appropriate surfactants. Supercritical fluid based microemulsions, emulsions, and latexes offer new opportunities in chemical manufacturing involving heterogeneous reactions (including polymerization), solvent free coatings, extraction of heavy metals including radioactive compounds from soils and waste water, polymer processing, and separations processes including cleaning and purification. The first generation of research involving surfactants in SCFs addressed reverse micelles and water-in-SCF microemulsions, for alkanes such as ethane and propane,[1−7] as reviewed recently.[8,9] The insight gained from these studies about phase equilibria, surfactant aggregation, interfacial curvature, and droplet interactions is directly applicable to microemulsions and emulsions in CO_2.

Carbon dioxide (T_c = 31 °C, P_c = 73.8 bar) is an attractive alternative to organic solvents because it is nontoxic, nonflammable, inexpensive, and environmentally benign. The properties of CO_2 are much different from those of water or nonpolar organic solvents. Unlike water, it has no dipole moment. Even when highly compressed, CO_2 has far weaker van der Waals forces than hydrocarbon solvents, as indicated by its low dielectric constant, ϵ, and polarizability per volume, α/v. Consequently, the most "CO_2-philic"[10] types of functional groups have low cohesive energy densities, e.g., fluorocarbons, fluoroethers, and siloxanes.[11−17] Nonvolatile lipophilic or hydrophilic phases are often insoluble in CO_2. Thus, CO_2 may be considered a third type of condensed phase. The appropriate choice of surfactant affords an opportunity to disperse either lipophilic[10,18] or hydrophilic phases[19−21] into CO_2, in the form of microemulsions, emulsions, and latexes. Examples of dispersed phases include PMMA latexes,[10] micelles with hydrated poly(ethylene glycol) cores,[19] and microemulsions with "bulklike" water cores, which were used to solubilize a protein, bovine serum albumen, in CO_2 for the first time.[20]

With polymeric steric stabilizers containing CO_2-philic groups,[10,22] it is even possible to perform heterogeneous polymerizations in SC-CO_2. The homopolymer poly(1,1-dihydroperfluorooctyl acrylate) PFOA stabilizes growing PMMA polymer particles in dispersion polymerizations of methyl methacrylate,[10] resulting in yields greater than 90% and molecular weights on the order of $M_n = 3 \times 10^5$. PMMA latex particles were produced with diameters from 1.55 to 2.86 μm.[23] More recently dispersion polymerizations of methyl methacrylate,[24] styrene,[18] and 2,6 dimethylphenol[25] in SC-CO_2 have produced high molecular weight products in high yields using multifunctional amphiphilic stabilizers.

The polymer, PFOA, is remarkably soluble in CO_2 at a level of 10 wt %.[26] With neutron scattering, it has been shown to have a positive second virial coefficient in dense CO_2,[17] indicating that CO_2 is a good solvent for this polymer at high densities. PFOA exhibits lower critical solution temperature (LCST) type phase behavior in CO_2.[23,26] The solvent quality of a supercritical fluid can be varied over a wide range through changes in density, by varying the temperature or pressure. As the density of the solution is lowered, CO_2 molecules leave the PFOA chains and expand into a new phase to raise the volume and entropy of the system. No longer solvated by CO_2, the PFOA molecules collapse.

[⊗] Abstract published in *Advance ACS Abstracts,* July 1, 1997.

S0024-9297(96)01693-2 CCC: $14.00

The mechanism of steric stabilization of emulsions and latexes has been studied extensively in liquid solvents,[27,28] and recently in SCFs by turbidimetry,[29] with theoretical models,[30] and polymerization studies.[10,23] Block copolymer stabilizers contain an "anchor" block that adsorbs to the dispersed phase and a "stabilizer" block with an affinity for the continuous phase. Provided the surface coverage by the surfactant is sufficient, emulsions or latexes will not flocculate as long as the stabilizer blocks are solvated and thus extended out into the solvent to overcome attractive van der Waals forces.[27] In supercritical and near-critical fluids, latexes flocculate when the continuous phase density (solvent quality) is decreased.[30,31] We designate the point of change in the stability of the emulsion with decreasing density as the critical flocculation density (CFD), in analogy to critical flocculation temperatures in liquid emulsions.

Recently, Peck combined the self-consistent field theory of Scheutjens and Fleer[32] with the lattice fluid theory[33] to produce a model of the structure and interactions of surfaces with anchored chains in compressible solvents, including supercritical fluids.[30] As two surfaces approach each other, the solvent leaves the interfacial region to increase the volume and entropy. This separation of solvent and chains during flocculation is analogous to LCST phase separation in bulk. According to Napper's mechanism[27] of steric stabilization by anchored polymeric chains, the flocculation temperature of a latex or emulsion corresponds directly to the Θ point for the "stabilizer" block in the bulk continuous phase.

The objective of this study is to understand the mechanism of steric stabilization and flocculation of emulsions in SC-CO_2 as a function of the molecular structure of the stabilizer, the stabilizer phase behavior, and the CO_2 density. Light scattering, specifically turbidimetry, is used to measure emulsion concentrations, emulsion stabilities, critical flocculation densities, and the reversibility of flocculation. The dispersed phase was a 92 K M_w poly(2-ethylhexyl acrylate) (PEHA); the homopolymer and block copolymer stabilizers were chosen due to a knowledge of the phase behavior of the stabilizer block PFOA,[17,23] and because of their success in dispersion polymerization.[10,23]

To provide a complete picture of the stabilization mechanisms, we utilize complementary measurements of interfacial tension (γ) with a tandem variable-volume pendant drop tensiometer[34] to characterize stabilizer adsorption and of emulsion droplet size by dynamic light scattering (DLS) in our companion study.[35] Three types of stabilization mechanisms are identified and compared for the three polymeric stabilizers. The direct study of emulsion stability by light scattering techniques is highly complementary to indirect studies, where the efficacy of the stabilizer is inferred from the properties of latex particles recovered from dispersion polymerizations. Advantages of the former technique include: emulsion stability measurements are direct and *in-situ*, the colloid and surface science may be separated from the polymerization kinetics, the solvent composition is fixed (since soluble monomer is not converted to dispersed polymer), and the molecular weight of the dispersed phase is fixed. The concepts developed in this study will not only be relevant for heterogeneous polymerizations but also be applicable to microemulsions and emulsions in a variety of other reaction, separation, and materials formation applications.

Theory

The turbidity τ is defined in terms of the attenuation of electromagnetic radiation at a scattering angle of 0 °

$$\tau = (1/l) \ln(I_o/I) \tag{1}$$

where l is the path length. The turbidity and the time dependence of the turbidity will be used to assess the concentration and stability of emulsions at a given temperature and pressure. When the droplet sizes are comparable to λ, as in the case of typical emulsions, τ can be obtained from the equation for specific turbidity

$$\tau = 3K^*c/2\rho D \tag{2}$$

where the scattering coefficient K^* can be calculated from Mie theory, c is the concentration of the dispersed phase, ρ is the dispersed phase density, and D is the droplet diameter. The scattering cross-section of an emulsion is dependent upon droplet size and distribution, wavelength, and refractive indices for the dispersed and continuous phases and may be calculated from Mie theory.[36,37]

If there is no repulsive barrier to flocculation, Brownian flocculation is fast and diffusion controlled, as described by Smoluchowski. Here it is assumed that sedimentation flocculation is negligible. The rate constant k is thus given by

$$k = 8\ k_B T/3\eta \tag{3}$$

where k_B is Boltzmann's constant and η is the viscosity of the medium. The bimolecular rate of flocculation of two identical droplets is described by second-order kinetics as

$$dc/dt = -kc^2 \tag{4}$$

where c is the concentration of droplets at time t. Integration of eq 4 yields the total concentration of single and double droplets.[38,39]

$$c = c_0/(1 + t/T_c) \tag{5}$$

where T_c, the time at which c will be half of c_0, is given by

$$T_c = 1/kc_0 \tag{6}$$

In the case where further flocculation leads to triple and higher order droplets, the total concentration is also given by eq 5.

With steric stabilization where a repulsive barrier is present, the rate constant for slow flocculation is given by $k_{slow} = k_{fast}/W$, where W is the stability ratio and k_{fast} is the rate constant in the Smoluchowski limit. The stability ratio is defined theoretically in terms of the interdroplet potential Φ as

$$W = 2R\int_{2R}^{\infty} \exp\left(\frac{\Phi}{k_B T}\right) r^{-2}\, dr \tag{7}$$

The potential has been calculated for spherical droplets with anchored chains in the lattice fluid self-consistent field theory.[30]

Experimental Section

Styrene (Aldrich), vinyl acetate (Aldrich), and 1,1-dihydroperfluorooctyl acrylate (3M) monomers were purified by pas-

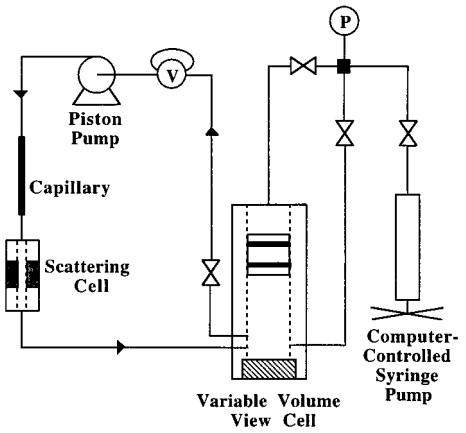

Figure 1. Schematic diagram of the turbidimetry apparatus.

sage through an alumina column and were deoxygenated by argon purge prior to use. Tetraethylthiuram disulfide (TD, Aldrich) was recrystallized twice from methanol. α,α′-Dichloro-*p*-xylene (Aldrich, 98%) and sodium *N*,*N*-diethyldithiocarbamate (Aldrich, 99+%) were used as received. Absolute alcohol and α,α,α-trifluorotoluene (Aldrich, 99+%) was used as received.

Synthesis of Poly(2-ethylhexyl acrylate) (PEHA). A 2 L reactor equipped with a stirrer, nitrogen purge, and monomer feed inlet was initially charged with 100 g of ethylhexyl acrylate (Aldrich Chemical Co.), 700 mL of toluene (Aldrich, HPLC grade), and 1.6 g of an initiator (azobis(isobutyronitrile), Vazo 67, DuPont). This initial mixture was purged with nitrogen for 30 min. The reactor temperature was raised to 75 °C to initiate polymerization. A further 100 g of ethylhexyl acrylate and 6.4 g of Vazo 67 in 15 mL of toluene was added in four aliquots over a 1 h period. The reaction was stopped by cooling the reaction mixture 5 min after the final reactant and initiator addition. Excess toluene was removed by evaporation, and residual solvent was removed in a vacuum oven at 50 °C for 48 h. From GPC, the M_w and M_n were 92K and 32K, respectively. The viscosity of the final product was estimated to be on the order of 10 000 P at ambient conditions and was reduced by several orders of magnitude when contacted with CO_2, based upon visual observation of stirring in the view cell.

Synthesis of PS-*b*-PFOA. Each of the stabilizers was synthesized at UNC. Polystyrene-*b*-PFOA diblock copolymers were synthesized using the "iniferter" technique developed by Otsu.[40] The synthesis of these specific block copolymers has been described previously.[16] The styrene block was synthesized first using TD as the iniferter. The telechelic PS block was then used as the macroinitiator in the photopolymerization of the second monomer, FOA, to form the second block of the diblock copolymer. The M_n of the PS block was determined by GPC prior to the addition of the FOA monomer. After the formation of the PFOA block, the ratio of FOA repeat units to styrene units was determined by ^{1}H NMR (see Table 2).

Synthesis of p-Xylene bis(*N*,*N*-diethyldithiocarbamate) (XDC). XDC was synthesized according to the literature.[41]

Synthesis of PFOA-*b*-PVAc-*b*-PFOA. The PVAc block was synthesized first using XDC as the iniferter. The telechelic PVAc block was then used as the difunctional macroinitiator in the photopolymerization of the second monomer, FOA, to give the PFOA-*b*-PVAc-*b*-PFOA triblock copolymer. As in the case of PS-*b*-PFOA, the M_n of the first block, PVAc, was determined by GPC prior to the addition of FOA monomer. After formation of the PFOA block, the ratio of FOA repeat units to vinyl acetate units was determined by ^{1}H NMR (See Table 2).

Phase Behavior and Turbidimetry. Emulsion stability experiments were performed at UT with PEHA dispersed in CO_2. The PEHA sample was a viscous liquid at room temperature and so was easily and reproducibly dispersed in CO_2. The apparatus setup is shown in Figure 1. An ISCO computer-controlled syringe pump (model 260D) containing pure CO_2 was used to control the system pressure, and a pressure transducer and digital readout (P) (Sensotech, model TJE/7039-01 and 060-3147-01, respectively) were used to monitor the system throughout the experiments. The pump was connected to a 1.75 cm i.d. variable volume view cell containing a piston[42] and an X-shaped magnetically-coupled stir bar. A Milton-Roy reciprocating miniPump (model NSI-33R; maximum flow rate = 8 mL/min) was used to mix, recirculate, and shear the contents of the system. The optical cell containing 1 cm thick sapphire windows had an aperture of 1.2 cm and a path length of 1.0 mm. A Beckman DU-40 UV−vis spectrophotometer connected to a PC was used to measure and collect turbidity data over time at set time intervals. Turbidity measurements were recorded at 5 s intervals at an incident wavelength of 450 nm.

The variable volume view cell was charged with known amounts of stabilizer and CO_2, which were mixed and recirculated until a homogeneous solution was obtained. The concentration of fluorinated polymer stabilizer in CO_2 was approximately 0.2 wt % (stabilizer/CO_2); selected experiments were also performed for stabilizer concentrations from 0.05 to 0.5 wt %. The phase boundary or cloud point for the polymer−CO_2 solution was determined visually and spectrophotometrically by reducing the system pressure to the point where the solution became turbid, indicating a two-phase system. The contribution to turbidity from the phase separation of the soluble polymers was found to be negligible relative to the turbidity due to the dispersed PEHA phase described below.

For all emulsion turbidity experiments a consistent amount of dispersed phase (3 wt % PEHA/CO_2) was introduced to the solution through a six-port sampling valve (V) (Valco model N6W). The shear necessary for emulsification was obtained by recirculating the heterogeneous mixture through a 5 cm long by 100 μm i.d. fused silica capillary. Emulsions were formed at a pressure well above the cloud point for the CO_2−stabilizer solution. The PEHA was dispersed into droplets by the magnetically coupled stir bar in the variable volume view cell and emulsified into small droplets during recirculation with the reciprocating pump. Recirculation was kept at a constant flow rate of about 4 mL/min for all experiments by adjusting the micrometer on the pump. After homogenization of the system contents for 15−20 min, recirculation and stirring were stopped and turbidimetry measurements were immediately started. After a period of time sufficient to obtain a steady decay rate at a given pressure (10−20 min), the pressure was quickly decreased (<10 s) without stirring or recirculation while turbidity measurements continued. A sequence of pressure drops was studied until the emulsion became unstable. This procedure provided consistently prepared emulsions for all tests and reproducible pressures where the emulsions became unstable. Most experiments were repeated at least twice for a given sample. After at least 1 h of shearing the sample, no significant change was observed in the turbidity or the decay curves. Some samples were exposed to cumulative shear times in excess of 2 h, with no loss in turbidity. This suggests the shear rate did not degrade the stabilizer or the dispersed phase for this exposure time.

Interfacial Tension Measurements. The tandem variable-volume pendant drop tensiometer described previously[34] was used to measure the interfacial tension between PEHA and CO_2 phases with and without stabilizer. The apparatus consisted of two variable volume view cells (the drop phase cell and the measurement cell), an optical rail for proper alignment, a light source, a video camera, and a computer. The measurement cell contained PEHA saturated with an excess amount of pure CO_2 and the drop phase cell contained pure CO_2 or CO_2−stabilizer solution. PEHA was used as the continuous phase because it wet the stainless steel tip if it was used as the drop phase.

Once a suitable drop was formed, timing of the drop age was started and several images were recorded as a function of drop age. Images of the drop were stored in Tagged Image File Format (TIFF) and the edge of the drop was extracted from data at various global threshold values using a C++ program. From the shape of the interface, the interfacial tension may be obtained using Laplace's equation

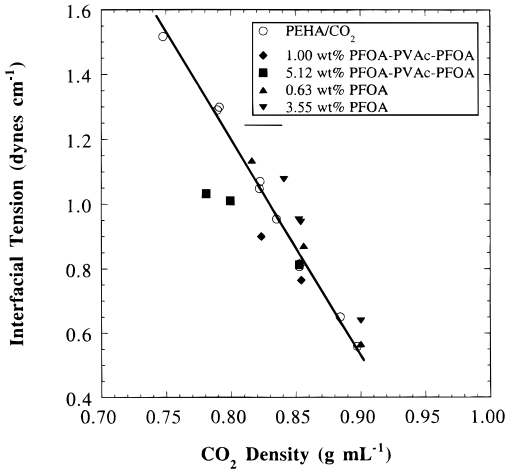

Figure 2. Interfacial tensions at 45 °C for the PEHA−CO_2 binary system, and systems including PFOA homopolymer and PFOA-*b*-PVAc-*b*-PFOA triblock copolymer. The total error is approximately ±0.05 dyn/cm.

$$\Delta P = \gamma(1/R_1 + 1/R_2) \tag{8}$$

where γ is the interfacial tension, R_1 and R_2 are the two principal radii of curvature, and ΔP is the pressure differential across the interface. Laplace's equation was expressed as a set of three first-order differential equations that were solved with a computer program to yield the interfacial tension.[43,44]

To determine γ from a pendant drop, it is necessary to know the densities of the two phases. The density of the PEHA phase saturated with CO_2 was measured using a Mettler-Paar DMA 512.[45] The temperature was controlled to ±0.1 degree with a water bath for the cell and a water jacket for the densitometer. Density measurements were made in both increasing and decreasing pressure with good agreement. Densities of the CO_2-rich phase were assumed to be equivalent to those of pure CO_2 and were obtained from Wagner's equation of state.[46]

Results and Discussion

PEHA in CO_2 Emulsions. Emulsions of PEHA in CO_2 without added stabilizer were studied to provide a baseline for the experiments below with added stabilizer. The concentration of the emulsion was determined from τ, and the emulsion stability was determined from the time dependence of τ. Mixtures of 1−3 wt % PEHA in CO_2 were introduced to the apparatus and emulsified. The amount of emulsion formed did not increase for PEHA loadings higher than 1 wt %, and the resulting turbidity was less than 20 cm^{-1}. Thus for the 3 wt % loading, about one-third of the PEHA was emulsified. The remainder of the PEHA, which had settled to the bottom of the variable volume cell, was continuously mixed and recirculated through the system. A small portion of the PEHA dispersed phase was soluble in CO_2 but had a negligible effect on the emulsion turbidity when pressure was decreased and the soluble fraction precipitated from CO_2.

To show why PEHA is so readily emulsified, measurements of interfacial tension γ between PEHA and CO_2 were made at 45 °C with the tandem variable-volume pendant drop tensiometer already referenced. The interfacial tension is quite low, on the order of 1 dyne cm^{-1} (see Figure 2). The combination of low interfacial tension and similar densities for CO_2 and PEHA phases[45] is responsible for the significant amount of emulsion formed in the binary system. The density difference ranges from a minimum of ∼0.15 g/mL at 174 bar and 25 °C to a maximum of ∼0.27 g/mL at 230 bar and 65 °C.[45]

Table 1. Emulsion Droplet Stabilities from Turbidimetry for PEHA in CO_2 Emulsions with Added Stabilizer

stabilizer	temp (°C)	cloud pt density (g/mL)	Θ-pt density (g/mL)	CFD (g/mL)	log(|dτ/dt|) @ ρ (g/mL)
PFOA	25	0.832	n/a	0.84	−3.3 @ 0.85
					−2.2 @ 0.83
					≫ −1.0 @ 0.81
PFOA	45	0.784	0.80	0.79	−3.6 @ 0.82
					−3.2 @ 0.79
					≫ −1.0 @ 0.76
PFOA	65	0.743	0.75	0.75	−3.3 @ 0.76
					−2.3 @ 0.74
					≫ −1.0 @ 0.73
PS-*b*-PFOA	25	0.835	n/a	0.86	−3.6 @ 0.85
					−3.1 @ 0.83
					−2.7 @ 0.81
PS-*b*-PFOA	45	0.790	0.80	0.80	−3.3 @ 0.82
					−3.0 @ 0.79
					−2.4 @ 0.76
PFOA-*b*-PVAc-*b*-PFOA	45	0.780	0.80	0.79	−2.3 @ 0.82
					−2.7 @ 0.79
					−2.2 @ 0.76

Emulsions with PFOA. Before injecting PEHA to form an emulsion, the cloud point of PFOA in CO_2 was measured. For a PFOA concentration of 0.25 wt %, the phase boundary is 108.3 bar (CO_2 density = 0.830 g/mL) at 25 °C. This result is consistent with the literature.[23] With two PFOA samples with molecular weights of 1×10^5 and 1.2×10^6, respectively, the cloud point densities were measured at a PFOA concentration of 0.73 wt %, which is close to the critical concentration.[23] Furthermore, in this region of the phase diagram, the cloud point density changes little with concentration. Thus the cloud point density is close to the density at the LCST. The Θ point densities for 45 and 65 °C were estimated by extrapolation of the cloud point densities at 0.73 wt % PFOA to infinite molecular weight (Table 1) and were within 0.003 g/mL of the LCST density for the nearly infinite molecular weight of 1.2×10^6. Phase behavior data were only available for two different molecular weight samples (1×10^5 and 1.2×10^6) with unknown polydispersities. It is noteworthy that the Θ point density estimated as above for 65 °C (0.75 g/mL) is significantly lower than the Θ point density determined from SANS measurements (0.81 g/mL).[47] This discrepancy is likely due to the polydispersity of the PFOA sample, and perhaps to the greater sensitivity of the SANS experiment to chain collapse at the onset of phase separation.

With 0.25 wt % PFOA dissolved in CO_2, essentially all of a 3 wt % PEHA sample is emulsified on the basis of turbidity measurements at various dispersed phase concentrations. The turbidity−time profiles for this 3 wt % PEHA in CO_2 emulsion stabilized with PFOA are shown in Figure 3 at 25 °C for four densities in sequence. At the highest CO_2 density (0.896 g/mL) the turbidity changes very little over 15 min indicating a very stable emulsion over this period of time. On this time scale, flocculation and sedimentation are negligible, and the stability of the emulsion is high, as defined by small values for $|d\tau/dt|$. The emulsion stability decreased slightly as the density was lowered to 0.838 g/mL, and much more substantially near the phase boundary for PFOA, 0.829 g/mL. With a very small further decrease in the density to 0.824 g/mL, the stability of the emulsion is significantly reduced. The slight increases in turbidity seen at each change in system pressure is mainly the result of the change in refractive index of the CO_2 continuous phase.

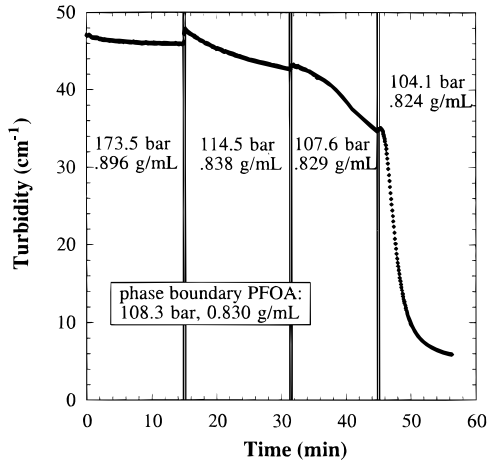

Figure 3. Turbidity−time profiles for a 3 wt % PEHA in CO_2 emulsion with 0.25 wt % PFOA homopolymer at 25 °C and various densities above and below the phase boundary for PFOA.

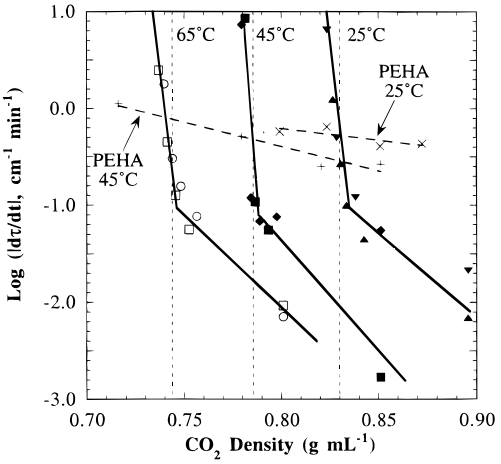

Figure 4. log |dτ/d*t*| versus density for 3 wt % PEHA in CO_2 emulsion with 0.25 wt % PFOA at 25, 45, and 65 °C. The vertical dotted lines represent the cloud point density for PFOA in CO_2 at various temperatures. The broad dashed lines are linear fits to the binary emulsion data at various temperatures.

For a given density, the stability |dτ/d*t*| was determined quantitatively from the initial slope of each decay curve excluding transients in the first few minutes. The trends in log of stability with density for PEHA emulsions with PFOA are plotted in Figure 4 for three temperatures. The vertical dotted lines denote the phase boundary for PFOA in CO_2 at each temperature. The broad dashed lines represent the stabilities of the PEHA emulsions without any added stabilizer. At densities well above the PFOA cloud point, the addition of PFOA greatly improves the stability of emulsions at each temperature. As the density is lowered very close to the phase boundary for PFOA, a sharp discontinuity in the slope of log |dτ/d*t*| is present. We denote this point the critical flocculation density (CFD) of the emulsion (Table 1). This change in the stability of the emulsion cannot be attributed to buoyancy or viscosity effects, on the basis of calculated sedimentation velocities and the lack of a change in slope for the PEHA emulsion without stabilizer. As the density is lowered below the CFD, PEHA emulsions with PFOA become much less stable than PEHA emulsions without PFOA. Here PFOA aids flocculation.

Direct determinations of effective stability factors (*W*) for these systems could not be obtained from |dτ/d*t*| with and without stabilizer. To determine *W*, the concentrations of the emulsions must be the same, but it was not possible to form a 3 wt % emulsion without stabilizer. It would be possible to determine *W* for a lower emulsion concentration.

Dynamic light scattering (DLS) experiments for dilute PEHA emulsions in CO_2 have been used to determine the effects of added stabilizers on droplets size and emulsion stability as reported in our companion study.[35] The apparatus and procedure for these experiments was similar to that used in the turbidimetry experiments. The only significant differences between the two sets of experiments were the concentrations of CO_2−soluble polymer and dispersed phase. DLS requires significantly lower concentrations to prevent multiple scattering effects from obscuring droplet size measurements. Thus, the concentrations used for DLS were approximately 0.05 wt % for both stabilizer and dispersed phase. Above the CFD, emulsion droplet sizes of approximately 500 nm are observed for PEHA emulsions with PFOA at 25 °C. As the density is decreased to the PFOA phase boundary, the emulsion droplets flocculate to yield sizes on the order of 1.5 μm. The DLS and turbidimetry experiments produced the same CFD, indicating that the CFD, does not depend significantly on the emulsion concentration.

The adsorption of polymer stabilizer at the PEHA−CO_2 interface is a key property for understanding emulsion stabilization and flocculation. The lowering of γ between PEHA and CO_2 as a function of the stabilizer concentration is a direct measure of the stabilizer adsorption. For the PFOA concentrations studied, the addition of PFOA homopolymer resulted in a slight increase in γ from the value for the PEHA−CO_2 binary system (Figure 2). This increase indicates that there is a slight negative excess, or depletion, of the homopolymer at the interface relative to bulk CO_2. The concentration of PFOA used in the turbidimetry was much lower than that used for interfacial tension experiments. The weak adsorption is indicative of a preference of PFOA for the CO_2 bulk phase relative to the interface, which is consistent with the positive second virial coefficient and high solubility of PFOA in CO_2.[17]

On the basis of droplet sizes determined from DLS and the turbidimetry stability measurements, we will now show that flocculation and sedimentation[48−50] each contribute to the loss in emulsion stability below the CFD. Sedimentation is the result of gravitational forces and may be calculated according to Stoke's law

$$t = 9\eta h/2\Delta\rho g r^2 \qquad (9)$$

where *t* is the sedimentation time, η is the continuous phase viscosity, *h* is the distance of fall of the droplets, $\Delta\rho$ is the density difference between the dispersed and continuous phases, and *r* is the droplet radius. For stable emulsions of PEHA in CO_2 at 25 °C and 104 bar, based on a measured density difference of 0.215 g/mL[45] and CO_2 viscosity of 7.69×10^{-4} P,[51] the time required for 500 nm diameter droplets to fall 0.5 cm (the distance from the top of our high-pressure optical cell to the turbidity measurement volume) is approximately 4 h. Thus, the high stabilities measured above the CFD are consistent with slow sedimentation of small droplets that do not flocculate.

Below the CFD, the following simple calculation shows that flocculation and sedimentation are highly coupled on the basis of the dτ/d*t* values. If it is assumed that there is no barrier to flocculation ($W = 1$) once the

CFD is crossed for PEHA emulsions with PFOA, flocculation may proceed at rates approaching Smoluchowski kinetics. This simple qualitative calculation neglects bridging flocculation, which will be shown to be operative for this system. For 3 wt % PEHA in CO_2 with a droplet radius of 250 nm, the initial droplet concentration is 4.6×10^{11} cm^{-3}, assuming monodisperse droplets. From eq 6, a characteristic time constant for flocculation of half of the single droplets, is 30 ms. The time scale for flocculation is orders of magnitude shorter than for sedimentation initially, but the rate of flocculation decreases rapidly as it is a function of the square of the droplet concentration. In contrast, the sedimentation time decreases with $1/r^2$. Eventually, both the rate of flocculation and sedimentation will become comparable in magnitude. By equating the sedimentation time calculated from eq 9 to the time for flocculation from eq 5, an approximate point of equivalence of the rates of flocculation and sedimentation may be determined. Polydispersity was not considered in this simple calculation. At 104 bar and 25 °C, the equivalence point occurs when the droplet size reaches approximately 3 μm, which occurs after only 70 s. This time frame is consistent with the time scale in the turbidity decay curves in Figure 3. Thus the flocculation and sedimentation rates are highly coupled.

The stabilization of emulsions by homopolymers in CO_2 may occur as a result of steric stabilization or depletion stabilization. For nonadsorbing polymers, emulsions may be stabilized by depletion forces.[28,52,53] As droplets approach each other, more solvent than polymer is squeezed out from between the surfaces, and the concentration of free polymer in this region increases. In a good solvent, this is energetically unfavorable. This concentration gradient sets up an osmotic pressure that resists flocculation.[28,52] It has been shown both experimentally[53−55] and theoretically[52] that stabilization of emulsions by nonadsorbing polymers generally occurs only at high stabilizer volume fractions, i.e., >0.05. In our experiments, the stabilities of the PEHA emulsions stabilized by PFOA were unchanged with PFOA concentrations from about 0.1 to 0.5 wt % when above the CFD. Because these concentrations appear to be too small for depletion stabilization to play a significant role, steric stabilization of the emulsion will be the dominant mechanism.

An increase in viscosity of the continuous phase would also decrease both the flocculation rate and sedimentation rate, as shown in eqs 3 and 9. The viscosity of the continuous phase would have to increase by a factor of roughly 100 to produce the increase in stability shown in Figure 4. Even for a PFOA concentration of 3.7 wt %, 6 times that in our study, the viscosity only increases by a factor of approximately 3.[47] This viscosity enhancement has little effect on emulsion stability.

The interfacial tension data and the change in emulsion stability with PFOA concentration will now be shown to support the steric stabilization mechanism. For steric stabilization a balance in the partitioning of the polymer between the continuous phase and the interface is required, as has been described for liquid solvents.[27] Sections of the homopolymer adsorb to the interface, called "trains"; the remainder is extended out into the continuous phase in closed "loops" between "trains" and in "tails" (see Figure 5). The solvent must be good in order to solvate the loops and tails to provide steric stabilization. Otherwise they will collapse and provide less steric repulsion, Figure 5. If the adsorption

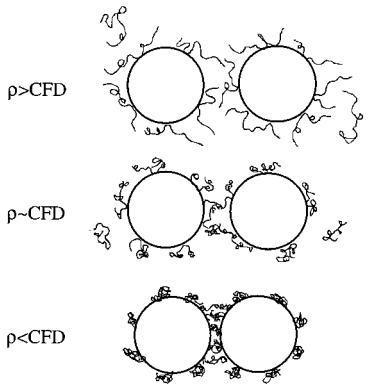

Figure 5. Schematic representation of the stabilization mechanism of PFOA for PEHA in CO_2 emulsions. The density of the continuous phase decreases from well above the CFD, to near the CFD, and finally to below the CFD.

to the interface is too strong, there will be a higher fraction of trains and insufficient loops and tails to provide steric repulsion.

The above interfacial tension data indicate that the number of PFOA segments that adsorb to PEHA in the form of trains covers only a small fraction of the surface, Figure 5. For 3 wt % PEHA dispersed in CO_2 with PFOA concentrations of 0.1−0.5 wt %, emulsions were stable above the CFD and essentially independent of concentration. The amount of surface coverage was sufficient enough to stabilize the emulsion. At a very low PFOA concentration of 0.05 wt %, the emulsions became considerably less stable for a given temperature and pressure. In this case, the small amount of surface adsorption was insufficient to protect enough of the PEHA surface with loops and tails for a stable emulsion to be obtained. From the various dispersed phase volume fractions, it appeared that a minimum stabilizer to PEHA mass ratio of about 1:30 was required to provide stability. These results agree qualitatively with literature data for the dispersion polymerization of MMA with PFOA, where product yields and molecular weights were shown to be essentially independent of PFOA concentration down to 0.0024 g of PFOA/g of MMA.[10,23]

Emulsions with the homopolymer PFOA present were significantly less stable than the binary PEHA−CO_2 emulsions below the CFD. After the emulsion had settled completely (i.e., $\tau < 2$ cm^{-1}), the system pressure was increased to raise the density of the CO_2 continuous phase well above the CFD. Even with PFOA present, visual observations of the emulsions in the view cell indicated that they could not be redispersed with the weak shear from the magnetically coupled stirrer. With the recirculation pump, essentially all of the system contents were redispersed.

Below the CFD, the flocculation of the emulsions may be caused by Hamaker forces between surfaces no longer separated by loops or tails, or by bridging of droplets by PFOA chains adsorbing to two or more surfaces. This multidroplet adsorption generally results in irreversible flocculation.[56] Higher molecular weight stabilizers are generally more prone to causing flocculation by a bridging mechanism, as they can more easily span the distance between two droplets. Above the CFD, bridging flocculation is limited as the adsorption of PFOA onto PEHA is small. The data in Figure 4 indicate clearly that flocculation below the CFD cannot be caused by the Hamaker forces alone. If flocculation were due only to the Hamaker forces, then the addition of PFOA

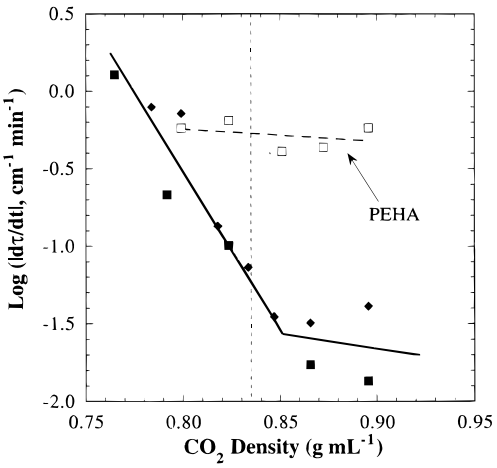

Figure 6. log |dτ/d*t*| versus density for 3 wt % PEHA in CO_2 emulsion with 0.10 wt % PS-*b*-PFOA at 25 °C. The vertical dotted line represents the cloud point density for PS-*b*-PFOA in CO_2. The broad dashed line is linear fit to the binary emulsion data.

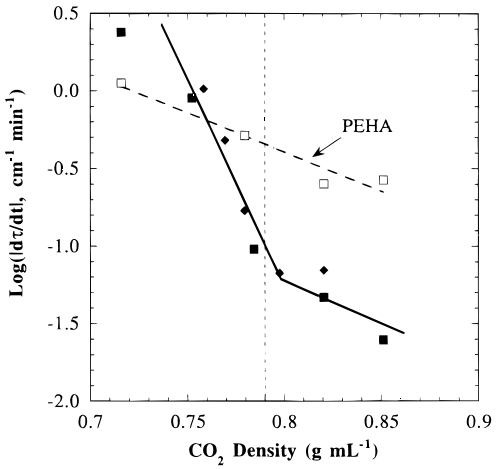

Figure 7. log |dτ/d*t*| versus density for 3 wt % PEHA in CO_2 emulsion with 0.10 wt % PS-*b*-PFOA at 45 °C. The vertical dotted line represents the cloud point density for PS-*b*-PFOA in CO_2. The broad dashed line is the linear fit to the binary emulsion data.

should not cause a great deal of destabilization of PEHA emulsions, as was observed. Adsorption of PFOA chains on PEHA is prevalent since the density is below the cloud point for PFOA. Many PFOA chains could be present in each floc as it grows. It is concluded, based on the enhanced and irreversible flocculation of the emulsion below the CFD, that the high molecular weight PFOA chains adsorb onto multiple droplet interfaces, resulting in bridging flocculation.

On the basis of the experimental results obtained from turbidimetry, complemented by those from tensiometry and DLS, we propose a mechanism for the stabilization and flocculation of PEHA emulsions by PFOA, as shown schematically in Figure 5. At high CO_2 densities the adsorbed PFOA extends out from the interface into the continuous phase. With a small fraction of the chain adsorbed to the interface (i.e., loops + tails ≫ trains), this high molecular weight homopolymer sterically stabilizes the emulsion. With a decrease in CO_2 density the PFOA chains begin to collapse but still enable steric repulsion to overcome the attractive interactions of the droplets. Below the CFD, the PFOA chains further collapse and can no longer overcome attractive forces between the droplets. Bridging flocculation ensues, due to the high molecular weight homopolymer adsorbing to multiple droplet interfaces, producing an irreversibly flocculated emulsion.

Emulsions with Polystyrene-*b*-PFOA. At high densities, the turbidity and turbidity versus time profiles for 3 wt % PEHA emulsions stabilized with PS-*b*-PFOA (4.5 K-*b*-24.5 K) were similar to those stabilized with PFOA. Figures 6 and 7 show plots for the log of |dτ/d*t*| versus CO_2 density at 25 and 45 °C, respectively. Again, the vertical dashed lines represent the cloud point for the polymeric stabilizer, and the broad dashed lines represent the stability of the binary emulsion. Because of the highly insoluble PS block, the cloud point is comparable to that for the PFOA homopolymer with a much higher molecular weight ($M_n \sim 1 \times 10^6$). As the density is lowered toward the phase boundary for PS-*b*-PFOA in CO_2, a discontinuity in emulsion stability is present, corresponding to the CFD. Below the CFD, the magnitude of the slope of log |dτ/d*t*| versus density is much smaller than for PFOA, indicating residual stabilization. Eventually, at very low densities, the emulsion becomes only modestly less stable than the binary emulsion without stabilizer. The degree of collapse versus temperature is sharp for infinite molecular weight but becomes more gradual as molecular weight decreases.

The results of DLS experiments for PS-*b*-PFOA stabilized PEHA emulsions[35] indicate droplet sizes consistently about 500 nm in diameter at densities above the copolymer phase boundary at 25 °C. The droplet sizes were the same as those for emulsions stabilized with PFOA. As the cloud point density for PS-*b*-PFOA was approached, droplet sizes increased by a factor of 2. When compared to emulsions stabilized with PFOA, neither the droplet sizes nor the scattering intensity dropped as rapidly. The trends in droplet sizes with density agree well with the trends in stability from turbidimetry.

Measurements of adsorption of PS-*b*-PFOA at the PEHA/CO_2 interface are not currently available. However, it may be expected to be highly interfacially active, since it adsorbs strongly at a similar interface, the PS/CO_2 interface.[35]

The ability of PS-*b*-PFOA to impart modest stability to the emulsion well below the CFD may be expected to influence the reversibility of flocculation. After the emulsion had completely settled out at a density below the CFD, the density was increased to well above the CFD. On the basis of visual observation in the view cell, the emulsion was easily and apparently completely redispersed with only low shear from the magnetically coupled stirrer. Even though flocculation had occurred, coalescence is not prevalent due to high surface coverage by PS-*b*-PFOA. Thus, even in the collapsed state, the PFOA blocks produce a short range repulsion that inhibits coalescence. If emulsions with PS-*b*-PFOA were left below the CFD for more than 1 h, the redispersability of the emulsion was significantly reduced. The flocculated state is only metastable with respect to the coalesced state. The loss of reversibility for the flocculated system over time is the result of the time required for the adsorbed polymer molecules to be expelled from the space between the flocculated droplets and for coalescence to occur.[27,49] After coalescence, the emulsion could only be redispersed by recirculating through the capillary tube.

The emulsion stability data may be used to test the predictions of the lattice-fluid self-consistent field model

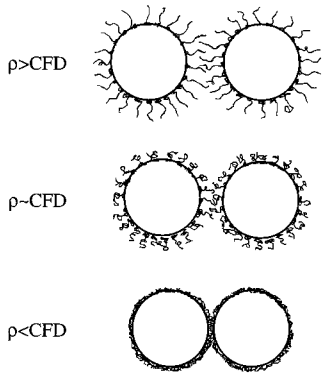

Figure 8. Schematic representation of the stabilization mechanism of PS-*b*-PFOA for PEHA in CO_2 emulsions. The density of the continuous phase decreases from well above the CFD, to near the CFD, and finally to below the CFD.

for interactions between surfaces with anchored chains in compressible solvents.[7,30] In its strictest sense the model is limited to polymer chains anchored to a surface, so that for a block copolymer the anchor block cannot leave the surface. Therefore, it is applicable to PS-*b*-PFOA but is not directly applicable to the PFOA homopolymer since it is not strongly anchored to the interface. The cohesive energy densities of PFOA and CO_2 may be expected to be very similar given the extremely high solubilities for this system. For systems in which the cohesive energy densities of the stabilizer and CO_2 are very similar, the model predicts that the CFD of the emulsion approaches the Θ point density of the stabilizer block in the bulk solvent, as we observed experimentally for the PS-*b*-PFOA and PFOA systems (Table 1).

The mechanism for stabilization of PEHA emulsions by PS-*b*-PFOA is presented in Figure 8. At high densities there is good surface coverage by the diblock copolymer, on the basis of the γ measurements, and the distended PFOA stabilizer blocks are able to overcome the attractive forces between droplets. With a decrease in density, the emulsion stability undergoes a discontinuity at the CFD, which occurs at the Θ point density for PFOA in CO_2. Below the CFD, flocculation is still much slower than for emulsions without stabilizer or emulsions stabilized by PFOA homopolymer. This residual stabilization is the result of the much higher surface coverage by PS-*b*-PFOA and by the lower molecular weight of the PFOA portion of the stabilizer. When the Θ point is reached, lower molecular weight PFOA collapses relatively less compared to higher molecular weight PFOA. This result suggests that block copolymers with high surface coverage can provide significant resistance to flocculation even below the CFD and that stabilization can be obtained with only moderate molecular weight stabilizers.

Emulsions with PFOA-*b*-PVAc-*b*-PFOA. This triblock copolymer PFOA-*b*-PVAc-*b*-PFOA has a 7.1 K molecular weight PVAc block that is designed to anchor to the PEHA interface, and two PFOA blocks of 100.6 K total molecular weight to sterically stabilize the emulsion. The addition of PFOA-*b*-PVAc-*b*-PFOA to emulsions of PEHA did not enhance emulsion stability at densities well above and well below the stabilizer cloud point (Figure 9). This copolymer enhanced the emulsion stability only in the proximity of the cloud point density. As the density is lowered toward the CFD, the stability actually increases and then decreases with density below the CFD. This interesting behavior was reproducible at a variety of PEHA concentrations

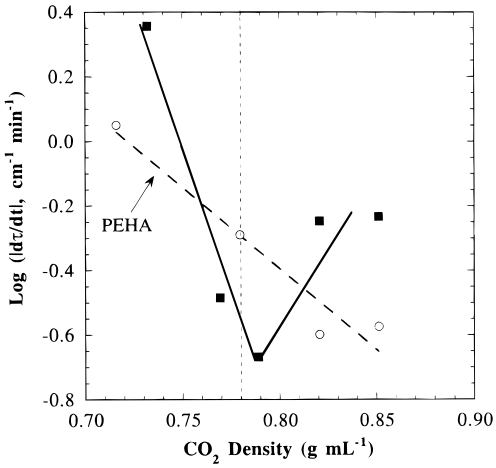

Figure 9. log |dτ/dt| versus density for 3 wt % PEHA in CO_2 emulsion with 0.27 wt % PFOA-*b*-PVAc-*b*-PFOA at 45 °C. The vertical dotted line represents the cloud point density of PFOA-*b*-PVAc-*b*-PFOA in CO_2. The broad dashed line is the linear fit to the binary emulsion data.

(1−5 wt % PEHA in CO_2) at 45 °C. At 25 °C however, PEHA emulsions with PFOA-*b*-PVAc-*b*-PFOA had stabilities similar to that of the binary emulsion, with no discernible trend in stability with density.

The interfacial tension measurements for PFOA-*b*-PVAc-*b*-PFOA at the PEHA−CO_2 interface echo the emulsion stability results. From Figure 2 it can be seen that at high CO_2 densities there is little change in γ from the PEHA−CO_2 binary system with the addition of PFOA-*b*-PVAc-*b*-PFOA. This indicates that there is little affinity of the triblock copolymer for the interface. It is known that PVAc and CO_2 interact more favorably than PS and CO_2 on the basis of their mutual solubilities,[57,58] and so PVAc likely will have limited affinity for the interface. Also, the high ratio of PFOA to PVAc further acts to keep the triblock copolymer solvated by CO_2 and away from the interface at high densities relative to PS-*b*-PFOA. It is surmised that the poor stabilization obtained at 25 °C was the result of the improved solvent strength of CO_2 at these conditions, causing even less adsorption at the PEHA−CO_2 interface.

The partitioning of PFOA-*b*-PVAc-*b*-PFOA between the CO_2 continuous phase and the interface changes dramatically as the density is lowered toward the phase boundary of the stabilizer in CO_2. As density is decreased toward the phase boundary for PFOA-*b*-PVAc-*b*-PFOA in CO_2, there is a continuous lowering of γ relative to the PEHA−CO_2 binary system. The triblock copolymer adsorbs more strongly to the interface when the solvation of the stabilizer blocks by CO_2 decreases. The increase in the stability of the emulsion to flocculation occurs in precisely the same density region where the stabilizer adsorption is the highest. As with PS-*b*-PFOA, the cloud point density of each PFOA block of the triblock copolymer will be significantly lower than the cloud point of the entire stabilizer, as PVAc is far less soluble in CO_2 than PFOA. In this case as well, the CFD corresponds very closely to the Θ point density for PFOA in pure CO_2, as expected from theory.

Below the CFD the emulsion became significantly less stable, but the magnitude of the slope of log |dτ/dt| versus density was still far smaller than for the homopolymer stabilizer, PFOA. Unlike the case for the stabilizer PFOA, the PS-*b*-PFOA-stabilized emulsion

Table 2. Relationship between Stabilizer Structure, Change in PEHA/CO_2 Interfacial Tension with the Addition of Stabilizer, and the Nature of the Flocculated Emulsion

stabilizer	anchor/stabilizer (M_n)	$\Delta\gamma$ (dynes/cm)	nature of flocculant
PFOA homopolymer	1×10^6 total	+0.12 average over all densities	irreversible
PS-*b*-PFOA	4.5 K/24.5 K	negative[a]	reversible
PFOA-*b*-PVAc-*b*-PFOA	7.1 K/100.6 K total	0 at high densities; −0.3 near CFD	partially reversible

[a] For 1850 M_n styrene dispersed phase.

was still more stable than the binary emulsion without stabilizer for a density range of ~0.03 g/mL and the flocculation of the emulsion was reversible. Compared with PS-*b*-PFOA, stabilization by PFOA-*b*-PVAc-*b*-PFOA was poorer at all densities and the flocculated state was less reversible, reflecting weaker surface adsorption at the PEHA−CO_2 interface (Table 2).

The mechanism of stabilization and flocculation for PEHA emulsions with PFOA-*b*-PVAc-*b*-PFOA reflects its varying interfacial activity with CO_2 density. At high densities there is little if any adsorption of this triblock copolymer at the interface. The resulting depletion and bridging flocculation cause the emulsion to be less stable than in the binary case without stabilizer. Depletion flocculation occurs at much lower polymer concentrations than depletion stabilization.[52−55] PFOA as well as PVAc can adsorb to the surface in bridging flocculation. As the phase boundary for the triblock copolymer is approached from higher densities, an increase in stability of the emulsion is observed due to steadily increasing amounts of triblock copolymer adsorbing at the interface. Below the CFD, the stability incurred by an increasing affinity of the triblock copolymer for the interface is lost as the stabilizer blocks collapse and can no longer provide steric stabilization. Bridging flocculation will also contribute to destabilization of the emulsion at densities well above and well below the CFD.

Conclusions

Turbidimetry offers a direct *in-situ* means to study mechanisms of emulsion stabilization and flocculation in supercritical fluids. For all stabilizers, the experimentally determined CFD is correlated well with the estimated Θ point density for PFOA determined from extrapolation of visual phase equilibria data to infinite molecular weight. This confirms the theoretical prediction of Peck[30] for emulsions in SCFs where the cohesive energy densities of the stabilizers and CO_2 are similar. For PEHA emulsions stabilized with PFOA homopolymer, the CFD was found to be close to the phase boundary for 1.2×10^6 PFOA in pure CO_2 as the molecular weight is essentially equivalent to infinite molecular weight. The weak adsorption of PFOA at the emulsion droplet interface indicates that steric stabilization is due to a high fraction of loops and tails extended into the CO_2 phase. Below the CFD, bridging flocculation results in rapid decay of the emulsion and irreversible flocculation. For PS-*b*-PFOA, significant stability is still imparted to the emulsion to densities well below the CFD relative to PEHA in CO_2 emulsions without stabilizer. Stabilization of the PEHA in CO_2 emulsion with PFOA-*b*-PVAc-*b*-PFOA block copolymer was only obtained at densities very close to the CFD as a result of increased adsorption at the interface. For all emulsion systems studied, there also exists a direct relationship between the interfacial activity of the stabilizer, the rate of flocculation below the CFD, and the reversibility of the flocculated state. This understanding of emulsion stabilization and flocculation is relevant to the design of surfactants for heterogeneous polymerizations, materials formation, and separation processes.

Acknowledgment. We acknowledge support from the NSF (CHE-9315329) (joint support to J.M.D. and K.P.J.), the Separation Research Program at the University of Texas, and Air Products & Chemicals. M.L.O. acknowledges support from the Natural Sciences and Engineering Research Council of Canada through postdoctoral funding. Thanks to Qiang Cao and Sanjay Kanakia for technical support. We also thank ISCO Corp. for the donation of the high-pressure syringe pump.

References and Notes

(1) Fulton, J. L.; Smith, R. D. *J. Phys. Chem.* **1988**, *92*, 2903−2907.
(2) Johnston, K. P.; McFann, G. J.; Lemert, R. M. In *Supercritical Fluid Science and Technology*; Johnston, K. P., Penninger, J. M. L., Eds.; ACS Symposium Series 406; American Chemical Society: Washington, DC, 1989; pp 140−164.
(3) Hoefling, T. A.; Enick, R. M.; Beckman, E. J. *J. Phys. Chem.* **1991**, *95*, 7127.
(4) McFann, G. J.; Johnston, K. P. *J. Phys. Chem.* **1991**, *95*, 4889.
(5) McFann, G. J.; Johnston, K. P. *Langmuir* **1993**, *9*, 2942−2948.
(6) Peck, D. G.; Johnston, K. P. *J. Phys. Chem.* **1991**, *95*, 9549−9556.
(7) Peck, D. G.; Johnston, K. P. *J. Phys. Chem.* **1993**, *97*, 5661.
(8) Bartscherer, K. A.; Renon, H.; Minier, M. *Fluid Phase Equilib.* **1995**, *107*, 93−150.
(9) McFann, G. J.; Johnston, K. P. In *Microemulsions: Fundamentals and Applied Aspects*; Kumar, P., Mittal, K. L., Eds.; Marcel Dekker: New York (in press).
(10) DeSimone, J. M.; Maury, E. E.; Menceloglu, Y. Z.; McClain, J. B.; Romack, T. J.; Combes, J. R. *Science* **1994**, *265*, 356.
(11) DeSimone, J. M.; Guan, Z.; Elsbernd, C. S. *Science* **1992**, *257*, 945.
(12) Hoefling, T. A.; Newman, D. A.; Enick, R. M.; Beckman, E. J. *J. Supercrit. Fluids* **1993**, *6*, 165−171.
(13) Newman, D. A.; Hoefling, T. A.; Beitle, R. R.; Beckman, E. J.; Enick, R. M. *J. Supercrit. Fluids* **1993**, *6*, 205−210.
(14) McHugh, M. A.; Krukonis, V. J. *Supercritical Fluid Extraction: Priciples and Practice*, 2nd ed.; Butterworth: Stoneham, MA, 1994.
(15) Harrison, K.; Goveas, J.; Johnston, K. P.; O'Rear, E. A. *Langmuir* **1994**, *10*, 3536−3541.
(16) Guan, Z.; DeSimone, J. M. *Macromolecules* **1994**, *27*, 5527−5532.
(17) McClain, J. B.; Londono, D.; Combes, J. R.; Romack, T. J.; Canelas, D. A.; Betts, D. E.; Wignal, G. D.; Samulski, E. T.; DeSimone, J. M. *J. Am. Chem. Soc.* **1996**, *118*, 917−918.
(18) Canelas, D. A.; Betts, D. E.; DeSimone, J. M. *Macromolecules* **1996**, *29*, 2818−2821.
(19) Fulton, J. L.; Pfund, D. M.; McClain, J. B.; Romack, T. J.; Maury, E. E.; Combes, J. R.; Samulski, E. T.; DeSimone, J. M.; Capel, M. *Langmuir* **1995**, *11*, 4241−4249.
(20) Johnston, K. P.; Harrison, K. L.; Clarke, M. J.; Howdle, S. M.; Heitz, M. P.; Bright, F. V.; Carlier, C.; Randolph, T. W. *Science* **1996**, *271*, 624−26.
(21) Singley, E.; Liu, W.; Beckman, E. J. *Fluid Phase Equilibr.* **1997**, *128*, 199−219.
(22) Adamsky, F. A.; Beckman, E. J. *Macromolecules* **1994**, *27*, 312−314.
(23) Hsiao, Y. L.; Maury, E. E.; DeSimone, J. M.; Mawson, S. M.; Johnston, K. P. *Macromolecules* **1995**, *28*, 8159−8166.
(24) Shaffer, K. A.; Jones, T. A.; Canelas, D. A.; DeSimone, J. M.; Wilkinson, S. W. *Macromolecules* **1996**, *29*, 2704−2706.

(25) Kapellen, K. K.; Mistele, C. D.; DeSimone, J. M. *Macromolecules* **1996**, *29*, 495−496.
(26) Luna-Barcenas, G.; Mawson, S.; Takishima, S.; Johnston, K. P. Submitted to *Fluid Phase Equilib.*
(27) Napper, D. H. *Polymeric Stabilization of Colloidal Dispersions*; Academic Press Inc.: New York, 1983.
(28) Fleer, G. T.; Cohen-Stuart, M. A.; Scheutjens, J. M. H. M.; Cosgrove, T.; Vincent, B. *Polymers at Interfaces*; Chapman and Hall: New York, 1993.
(29) O'Neill, M. L.; Yates, M. Z.; Johnston, K. P.; Wilkinson, S. P.; DeSimone, J. M. *Polym. Mater. Sci. Eng.* **1996**, *74*, 228−229.
(30) Peck, D. G.; Johnston, K. P. *Macromolecules* **1993**, *26*, 1537.
(31) Everett, D. H.; Stageman, J. F. *Faraday Discuss. Chem. Soc.* **1978**, *65*, 230−241.
(32) Scheutjens, J. M. H.; Fleer, G. J. *J. Phys. Chem.* **1979**, *83*, 1619.
(33) *Physics of Polymer Surfaces and Interfaces*; Sanchez, I. C., Ed.; Butterworth-Heinemann: Boston, 1992.
(34) Harrison, K. L.; Johnston, K. P.; Sanchez, I. C. *Langmuir* **1996**, *12*, 2637−2644.
(35) Yates, M. Z.; O'Neill, M. L.; Johnston, K. P.; Webber, S.; Canelas, D. A.; Betts, D. E.; DeSimone, J. M. *Macromolecules* **1997**, *30*, 5060−5067 (following article in this issue).
(36) Heller, W.; Pangonis, W. J. *J. Chem. Phys.* **1957**, *26*, 498−506.
(37) Melik, D. H.; Fogler, H. S. *J. Colloid Interface Sci.* **1983**, *92*, 161−180.
(38) Sheludko, A. *Colloid Chemistry*; Elsevier: New York, 1966; pp 277.
(39) Vera, P.; Gallardo, V.; Salcedo, J.; Delgado, A. V. *J. Colloid Interface Sci.* **1996**, *177*, 553−560.
(40) Otsu, T.; Yoshida, M. *Makromol. Chem., Rapid Commun.* **1982**, *3*, 127.
(41) Otsu, T.; Kuriyama, A. *Polym. Bull.* **1984**, *11*, 135.
(42) Lemert, R. M.; Fuller, R. A.; Johnston, K. P. *J. Phys. Chem.* **1990**, *94*, 6021−6028.
(43) Rotenberg, Y.; Boruvka, L.; Neumann, A. W. *J. Colloid Interface Sci.* **1983**, *93*, 169−183.
(44) Jennings, J. W.; Pallas, N. R. *Langmuir* **1988**, *4*, 959−967.
(45) Harrison, K. L. Ph.D. Dissertation, University of Texas at Austin, 1996.
(46) Ely, J. F. *CO_2PAC A Computer Program to Calculate the Properties of Pure CO_2*; National Bureau of Standards; Boulder, CO, 1986.
(47) McClain, J. B.; Betts, D. E.; Canelas, D. A.; Samulski, E. T.; DeSimone, J. M.; Londono, J. D.; Wignall, G. D. *Polym. Mater. Sci. Eng.* **1996**, *74*, 234−5.
(48) Reddy, S. R.; Fogler, H. S. *J. Colloid and Interface Sci.* **1981**, *79*, 105−113.
(49) Tadros, T. F.; Vincent, B. In *Basic Theory*; Becher, P., Ed.; Encyclopedia of Emulsion Technology, Vol. 1 Marcel Dekker, Inc.: New York and Basel, 1983; pp 129−286.
(50) Melik, D. H.; Fogler, H. S. In *Basic Theory Measurement Applications*; 1st ed.; Becher, P., Ed.; Marcel Dekker: New York and Basel, 1988; Vol. 3; pp 3−78.
(51) Vesovic, V.; Wakeham, W. A.; Olchowy, G. A.; Sengers, J. V.; Watson, J. T. R.; Millat, J. *J. Chem. Ref. Data* **1990**, *19*, 763−808.
(52) Feigin, R. J.; Napper, D. H. *J. Colloid Interface Sci.* **1980**, *75*, 525−541.
(53) Sober, D. L.; Walz, J. Y. *Langmuir* **1995**, *11*, 2352−2356.
(54) Biggs, S.; Milling, A. *J. Colloid Interface Sci.* **1995**, *170*, 604−606.
(55) Meller, A.; Stavans, J. *Langmuir* **1996**, *12*, 301−304.
(56) Adachi, Y. *Adv. Colloid Interface Sci.* **1995**, *56*, 1−31.
(57) Berens, A. R.; Huvard, G. S. In *ACS Symposium Series: Supercritical Fluid Science and Technology*; Johnston, K. P., Penninger, J. M. L., Eds.; American Chemical Society: Washington, DC, 1989; Vol. 406; pp 207−223.
(58) Rindfleisch, F.; DiNoia, T.; McHugh, M. *Polym. Mat. Sci. Eng.* **1996**; *74*, 178.

MA9616930